Original Article

Potential utility of miRNAs derived from pleural fluid extracellular vesicles to differentiate between benign and malignant pleural effusions

Tian Mun Chee[1]^, Caeli J. Zahra[1]^, Kwun M. Fong[1,2]^, Ian A. Yang[1,2]^, Rayleen V. Bowman[1,2]

[1]The University of Queensland Thoracic Research Centre, The Prince Charles Hospital, Brisbane, Australia; [2]Department of Thoracic Medicine, The Prince Charles Hospital, Brisbane, Australia

Contributions: (I) Conception and design: TM Chee, KM Fong, IA Yang, RV Bowman; (II) Administrative support: TM Chee; (III) Provision of study materials or patients: TM Chee, KM Fong, IA Yang, RV Bowman; (IV) Collection and assembly of data: TM Chee, CJ Zahra; (V) Data analysis and interpretation: TM Chee, CJ Zahra, RV Bowman; (VI) Manuscript writing: All authors; (VII) Final approval of manuscript: All authors.

Correspondence to: Tian Mun Chee, PhD. The University of Queensland Thoracic Research Centre, The Prince Charles Hospital, 627 Rode Road, Chermside, Brisbane, Queensland 4503, Australia. Email: t.chee@uq.edu.au.

Background: Cytological examination is of suboptimal sensitivity but high specificity for the diagnosis of malignant pleural effusions (MPEs). Pleural fluid extracellular vesicles (PFEVs) are enriched with disease-specific microRNAs (miRNAs) which may improve the diagnostic yield for MPE. Our previous study demonstrated the feasibility of isolating miRNAs from PFEVs and profiling PFEV miRNAs by Nanostring nCounter® Human v3 miRNA expression assay. Here, we interrogated in a small cohort to evaluate the diagnostic potential of PFEV miRNAs to differentiate between benign pleural effusion and MPE.

Methods: Extracellular vesicles (EVs) from pleural fluids were isolated by two sequential ultracentrifugation steps. PFEVs were extracted and characterised by western blotting analysis, particle analysis by tunable resistive pulse sensing (TRPS) technology, and transmission electron microscopy (TEM). Total RNAs (including miRNAs) were extracted from PFEVs and profiled by the Nanostring nCounter® 827 probe miRNA expression assay. Differential expression analysis of the miRNA expression assays on PFEV samples was performed using the Bioconductor DESeq2 package.

Results: EVs from pleural fluids were evident by staining of positive EV-associated protein markers, particle size distribution within the expected parameters, and the cup-shaped morphology by TEM. Employing Nanostring nCounter® Human v3 miRNA expression assay, this proof-of-principle study demonstrated PFEV miRNAs were differentially expressed between benign effusions and malignant effusions [malignant pleural mesothelioma (MPM) or lung adenocarcinoma metastatic to pleura (metLUAD)]. The expression of six miRNAs (hsa-miR-1246, hsa-miR-136-5p, hsa-miR-141-3p, hsa-miR-145-5p, hsa-miR-200c-3p, and hsa-miR-9-5p) significantly differed between benign and malignant effusions, or between MPM and metLUAD, at adjusted $P<0.05$ and $\log_2$fold change ≥ 1.0.

Conclusions: The miRNAs identified from this study could be interrogated further for their utility as a single biomarker candidate or to be tested simultaneously in a panel to complement pleural effusion diagnostics. PFEV miRNAs represent a novel bioresource with potential to aid in the diagnosis of pleural effusions. Larger prospective studies are needed to confirm their diagnostic utility.

Keywords: Pleural fluid; extracellular vesicles (EVs); microRNA (miRNA); lung cancer; mesothelioma

^ ORCID: Tian Mun Chee, 0000-0002-9320-0487; Caeli J. Zahra, 0009-0004-4256-0644; Kwun M. Fong, 0000-0002-6507-1403; Ian A. Yang, 0000-0001-8338-1993.

Submitted Oct 17, 2024. Accepted for publication Dec 19, 2024. Published online Jan 22, 2025.
doi: 10.21037/tlcr-24-945
View this article at: https://dx.doi.org/10.21037/tlcr-24-945

Introduction

Pleural effusion in adults may arise due to benign or malignant conditions affecting the pleura (1). Even in the absence of previously known cancer, malignancy is the most common cause of large unilateral effusion in adults. Malignant disease of the pleura may arise in pleura itself, as in malignant pleural mesothelioma (MPM) or it may occur with direct invasion of pleura by tumours in adjacent lung, or from metastases to pleura from primary tumours originating in remote sites such as breast or ovary.

Diagnostic testing of pleural fluid obtained at thoracentesis includes microscopy and culture for pathogenic organisms on unprocessed pleural fluid, biochemical analyses for pH, glucose, protein, and enzyme levels in the cell-free fraction after low-speed centrifugation, differential cell counts, light microscopy and immunohistochemistry on cell blocks prepared from the centrifugation pellet (2). Pleural fluid cytology is heavily relied upon to differentiate benign from malignant effusions, and has overall sensitivity of 40–80% and specificity 89–98% for malignancy in general, including high sensitivity (HS) for lung adenocarcinoma metastatic to pleura (metLUAD) at 88% (2-4). There are well-recognized difficulties with the cytological diagnosis of certain tumours that cause pleural effusion, especially non-epithelial malignancies such as MPM, for which pleural fluid cytology has low sensitivity, and cytology alone is non-diagnostic in 55–70% of cases (4).

Extracellular vesicles (EVs) have an orchestrated biosynthesis and are released from all cell types into body fluids (5,6). EVs have a lipid bilayer enclosure, no functioning nucleus, and contain DNA, RNA, characteristic proteins, and other biomolecules. They are postulated to maintain cellular homeostasis by removing unnecessary or excessively produced biomolecules from host cells, to facilitate intercellular communication by transferring contents to recipient cells, and in some cases to exert effects in recipient cells by transferring oncoproteins, oncomirs, and non-coding RNAs, imposing gene regulation on recipient cells at post-transcriptional level (7,8).

MicroRNAs (miRNAs) packaged into EVs have previously been reported as potentially useful cancer diagnostic markers in pleural effusions (9,10). In patients with metLUAD, EV-derived miRNAs isolated from pleural effusions comprised over 40% of EV total RNA, whereas in effusions associated with pneumonia and pulmonary tuberculosis, the miRNA fraction is lower (11). The diagnostic potential of tumour tissue-derived miRNAs has been demonstrated by The Cancer Genome Atlas (TCGA) pan-cancer study, in which miRNA analysis in 21 cancer types led to the establishment of an open-source web tool capable of diagnosing cancers with 97.2% overall accuracy, subsequently validated in independent datasets with high specificity and sensitivity (12). In malignant pleural effusions (MPEs), selective packaging of components into pleural fluid EVs (PFEVs) cargo, including enrichment of specific miRNAs, presents a novel bioresource with diagnostic potential to distinguish between malignant and non-malignant (NM) effusions, and between specific types of malignant pleural diseases. Thus far, no study has reported differentially expressed miRNAs derived from PFEVs that distinguish MPE due to benign causes, MPM and metLUAD.

We previously demonstrated successful isolation of EVs from pleural fluid and optimised methods for EV miRNA

Highlight box

Key findings
- Extracellular vesicles (EVs) in pleural fluids facilitate differential diagnosis.
- MicroRNAs (miRNAs) from pleural fluid EVs (PFEVs) differentiate between benign and malignant pleural effusions.

What is known and what is new?
- Standard diagnostic tests based on cellular and supernatant fractions of pleural effusion currently have suboptimal diagnostic test characteristics for the diagnosis of pleural disease.
- miRNAs packaged into EVs have previously been reported as potentially useful cancer diagnostic markers in pleural effusions.
- miRNA candidates could be explored further as a single biomarker candidate to differentiate different pleural effusion diseases or to be tested simultaneously in a panel to complement current pleural effusion cytological testing.

What is the implication, and what should change now?
- miRNAs from PFEVs present as a novel bioresource in cytology diagnostics.

profiling (13). Here, we report on the feasibility of profiling PFEV miRNAs using the Nanostring nCounter® miRNA expression assay in a cohort of 29 cases. We identified PFEV miRNAs with significant differential expression between malignant and benign effusions, and between MPM and metLUAD. We conclude that further investigation in larger prospective studies could help define the diagnostic utility of PFEV miRNA analysis in pleural diseases. We present this article in accordance with the MDAR reporting checklist (available at https://tlcr.amegroups.com/article/view/10.21037/tlcr-24-945/rc).

Methods

Patient consent

The present study was directed in accordance with the guidelines of the Declaration of Helsinki (as revised in 2013). Patients who underwent thoracentesis gave written informed consent to donate pleural fluid remaining after diagnostic pathology examination to The Prince Charles Hospital Lung Bank (approval number: HREC/17/QPCH/54), approved by the Metro North Health Human Research Ethics Committee. This study, including approval to access the specimens collected through The Prince Charles Hospital Lung Bank, was approved by the Metro North Health Human Research Ethics Committee (approval number: LNR/2019/QPCH/52409) and The University of Queensland Human Ethics Research Committee (approval number: 2019001147/HREC/52409), with access to retrospectively collected specimens under The Prince Charles Hospital Lung Bank.

Isolation of PFEV

Pleural fluid was centrifuged at 600 ×g for 7 minutes to pellet the cellular fraction, and the supernatant (cell-free pleural fluid) was stored at –80 ℃. The thawed cell-free pleural fluid was sieved through a 40 µm cell strainer (DKSH, Victoria, Australia; Cat. No. 15-1040-1) to remove tissue fragments, blood clots, and large particles. Filtrate was centrifuged at 800 ×g for 10 minutes at 4 ℃. Sixteen mL of cell-free pleural fluid was then subjected to two sequential ultracentrifugation at 100,000 ×g (w^2t = 5.46e10) for 1 hour 40 minutes (each spin) at 4 ℃ using a Beckman Optima XPN-100 ultracentrifuge, and 50.2 Ti rotor (Beckman Coulter, IN, USA). The pellet resulting from the final ultracentrifugation was used for RNA extraction.

Western blotting

Micro BCA Assay (Thermo Fisher Scientific, Waltham, MA, USA; Cat. No. 23235) was used to quantify the protein content in PFEV. 1.5 µg of protein was stained against EV-associated protein markers—positive (CD9, flotillin-1); negative (albumin). Samples were prepared with 10 µL Bolt LDS Sample Buffer (4×) and 4 µL Bolt Reducing Agent. The mixture was heated at 70 ℃ for 10 minutes, then placed on ice for a further 10 minutes. Gel electrophoresis was performed at 90 V for 90 minutes, followed by western blot transfer at 25 V for 6 minutes over iBlot 2 Gel Transfer Device. The blot was then blocked for 30 minutes in tris-buffered saline supplemented with 0.1% Tween (TBS/0.1% Tween) and 5% skim milk powder. Novex™ Sharp Pre-Stained Protein Standard (Thermo Fisher Scientific; Cat. No. LC5800) was used on all blots. Primary antibody incubation was performed as follows: anti-albumin (1 hour; 1:1,000; Cell Signaling Technology, Danvers, MA, USA; Cat. No. 4929S; RRID:AB_2225785), anti-flotillin-1 (D2V7J) XP® rabbit monoclonal antibody (mAb) (overnight; 1:1,000; Cell Signaling Technology; Cat. No. 18634S; RRID:AB_2773040), and anti-CD9 (D8O1A) rabbit mAb (overnight; 1:2,000; Abcam, Cambridge, UK; Cat. No. EPR2949; RRID:AB_10561589). The blot was then incubated in goat anti-rabbit immunoglobulin G (IgG) (H + L) secondary antibody, horseradish peroxidase (HRP) (1:10,000; Thermo Fisher Scientific; Cat. No. 31460; RRID:AB_228341) for an hour. TBS/0.1% Tween wash was performed between blocking and antibody incubations. Finally, flotillin-1 and CD9 blot strips were developed using SuperSignal™ West Femto Maximum Sensitivity Substrate (Thermo Fisher Scientific; Cat. No. 34094), whereas albumin blot strip was developed using Novex enhanced chemiluminescence (ECL) HRP chemiluminescent substrate (Thermo Fisher Scientific; Cat. WP20005) for 5 minutes, and detected over ChemiDoc™ MP imaging system (Bio-Rad, Hercules, CA, USA).

Transmission electron microscopy (TEM)

PFEV visualisation by TEM was outsourced to The University of Queensland Centre for Microscopy and Microanalysis (UQCMM). Negative staining was performed on undiluted PFEV on Formvar filmed, carbon-coated and flow-discharged electron microscopy (EM) grids. Images were acquired with a JEOL JEM-1011 TEM operated at 100 kV equipped with a SIS Morada Camera,

and acquisition software Olympus iTEM 5.2 at scale bars of 2, 1, and 0.5 µm (500 nm).

Tunable resistive pulse sensing (TRPS)

Two representative PFEV samples—PF6238 and PF6246, were analysed by The Exoid analyzer (Izon Science Ltd., Christchurch, NZ, New Zealand). NP100 and NP600 nanopores (CP100 and CP800 calibration particles) were used, with the samples measured at three different pressure settings (400, 600, and 1,000 Pa). Respectively, the target particle size range for NP100 and NP600 were 50–330 and 272–1,570 nm. Data and graphs for the size distribution of PFEV samples were generated from The Izon Data Suite (software version 1.0.2.32).

Total RNA extraction and miRNA assessment

Total RNA was extracted according to the manufacturer's instructions using Qiazol reagent (Qiagen, Hilden, NRW, Germany; Cat. No. 79306) and Norgen RNA Clean-Up and Concentration Micro-Elute Kits (Norgen Biotek Corp., Thorold, ON, Canada; Cat. No. 61000), following protocol B (96–100% ethanol in step 1b). Briefly, PFEV pellet (from the final ultracentrifugation) was re-suspended in 0.5–0.7 mL of Qiazol reagent. The mixture was homogenised and incubated at room temperature for 5 minutes. One hundred and forty µL of chloroform was added and the mixture was incubated at room temperature for 3 minutes and spun at 12,000 ×g for 15 minutes at 4 ℃. After separation of aqueous and organic phases, the upper aqueous phase containing RNA was collected into a new RNase-free microtube. Three hundred and fifty µL 100% ethanol was added and this was followed by column washes according to manufacturer's instructions. Total RNA was eluted in 10 µL of elution buffer. The extracted total RNA was then assessed by Qubit™ HS RNA assay (Thermo Fisher Scientific; Cat. No. Q32852) and Bioanalyzer Small RNA assay (Agilent, Santa Clara, CA, USA; Cat. No. 5067-1548) prior to miRNA expression assay.

Nanostring miRNA expression assay

The Nanostring nCounter® Human v3 miRNA expression assay panel includes 798 miRNA probes to screen 827 miRNAs that are highly curated in miRBase 22 (released 12th March 2018). Unique oligonucleotide tags were ligated onto native miRNAs in a total RNA sample, followed by hybridisation (12–30 hours) of tagged miRNAs and capture/reporter probes with colour-coded sequence specific to each miRNA target. The assay was performed following nCounter miRNA Expression Assay user manual (MAN-C0009-07; v. April 2018). Post-hybridisation samples were then loaded onto a SPRINT cartridge (NanoString Technologies, Inc., Seattle, WA, USA; Cat. No. 100078) and processed on the Nanostring nCounter® SPRINT Profiler (NanoString Technologies, Inc.). Data was acquired through instrument automated fluorescence microscope scanning with direct counts of target-probe complexes and analysed by Nanostring nSolver™ software (version 4.0.70).

Statistical and bioinformatics data analysis

Differential expression analysis of the miRNA expression assays on PFEV samples was performed using the Bioconductor DESeq2 package (14), applying default parameters and the Benjamini-Hochberg correction. R package ggplot2 was applied to generate boxplots of miRNA raw or normalised expression data.

Results

Patient characteristics

We tested pleural fluid samples from 29 participants: 8 females and 21 males, aged 49 to 99 years (median, 71 years) at the time of thoracentesis. Twenty-two cases had malignant effusions: 11 with MPM, and eleven with metLUAD. Seven cases were due to NM conditions, including parapneumonic effusions, inflammatory pleuritis or benign asbestos-related pleural effusions (*Table 1*). Cases diagnosed with benign conditions after tissue biopsy or surgical resection underwent prolonged (at least 6 months) clinical follow-up to confirm that they were not subsequently diagnosed with malignancy.

The final diagnoses were established by pleural fluid cytology, or histopathology of pleura obtained by biopsy or surgical resection. Pleural fluid analysis alone provided a definitive diagnosis in seven cases (MPM, n=1; metLUAD, n=2; NM, n=4), and pleural biopsy alone was diagnostic in ten cases (MPM, n=8; metLUAD, n=2). Definitive diagnosis was made from both pleural fluid analysis and biopsy in ten cases (MPM, n=2; metLUAD, n=5; NM, n=3). Two metLUAD cases were confirmed from surgical resection lung histopathology demonstrating tumour invading pleura.

Table 1 Demographic data of 29 pleural fluid donors

Variables	MPM (n=11)	MetLUAD (n=11)	NM (n=7)	Overall (n=29)
Sex, n				
Female	1	7	0	8
Male	10	4	7	21
Age (years), median [min, max]	71 [59, 89]	64 [49, 84]	80 [52, 99]	71 [49, 99]
Final diagnostic specimen, n				
Pleural fluid	Epithelioid: 1	2	4	7
Pleural biopsy	Epithelioid: 5	2	–	10
	Sarcomatoid: 2	–	–	–
	Biphasic: 1	–	–	–
Both pleural fluid and biopsy	Biphasic: 2	5	3	10
Surgical lung biopsy/resection	–	2	–	2

Donors were 8 females and 21 males, age ranging from 49 to 99 years (median age, 71 years). The final diagnoses based on pleural fluid cytology, pleural biopsy or surgical tissue histology of the 29 effusions were MPM (n=11), metLUAD (n=11), and NM conditions (n=7). MPM, malignant pleural mesothelioma; metLUAD, lung adenocarcinoma metastatic to pleura; NM, non-malignant.

Characterisation of EVs isolated from pleural fluid

EV characterisation was performed on two randomly selected samples—PF6238 (metLUAD) and PF6246 (NM). Western blot analysis showed positive staining with EV-characterising primary antibodies at varying intensity (*Figure 1A*). Both cases demonstrated comparable expression of albumin and flotillin-1, whereas PF6238 stained stronger for CD9 than PF6246. TRPS analysis of these samples showed an overall particle size distribution ranging from 80 to 520 nm. Analysis with NP600 showed average particle size distribution of 440±136 nm for PF6238 and 451±141.6 nm for PF6246. With NP100, the average size distribution was observed at 99±26.4 nm (PF6238) and 105±38.5 nm (PF6246) (*Figure 1B*). Finally, EVs with typical cup-shaped morphology were evident by TEM analysis in both samples (*Figure 1C*).

PFEV RNA yield was heterogeneous for PFEV samples

Figure 2A shows the amount of RNA (per mL of pleural fluid expressed in Log_2 transformed values) extracted from 29 PFEV samples, as assessed by Qubit HS RNA and Bioanalyzer Small RNA assays. The amount of total RNA measured by Qubit HS RNA assay ranged from 1.38 to 14.63 ng per mL of pleural fluid volume used for EV isolation. In Bioanalyzer Small RNA assay, data for miRNA and small RNA contents were available for each sample measured. Expressed as per mL of pleural fluid volume used for EV isolation, the range of miRNA contents from 29 PFEVs was from 0.58 to 491.36 µg, whereas the small RNA contents ranged from 1.23 to 2900.72 µg. Detailed quantification results from both Qubit and Bioanalyzer assays were accessible through supplementary datasets (https://doi.org/10.48610/cece534).

Bioanalysis of RNA content from ten randomly selected PFEVs is illustrated in *Figure 2B*. Band sizes observed on the electrogram of Bioanalyser miRNA assay ranged from 4 to 150 nucleotides at varying intensities.

Nanostring nCounter® miRNA expression assay performance in PFEV samples

The performance of Nanostring nCounter® miRNA expression assays was indicated by the expression of internal control probes. Background signal of eight negative control probes (A–H) was low in all samples (*Figure 3A*). Positive control probes A–F [synthetic messenger RNA (mRNA) targets at specified concentrations] showed consistent loading of input amount, and minimal lane-to-lane variation (*Figure 3B*). As expected in total RNA extracted from PFEV, endogenous mRNA targets commonly expressed in biological samples were detected by the mRNA reference control probes including ACTB, B2M, GAPDH, RPL19,

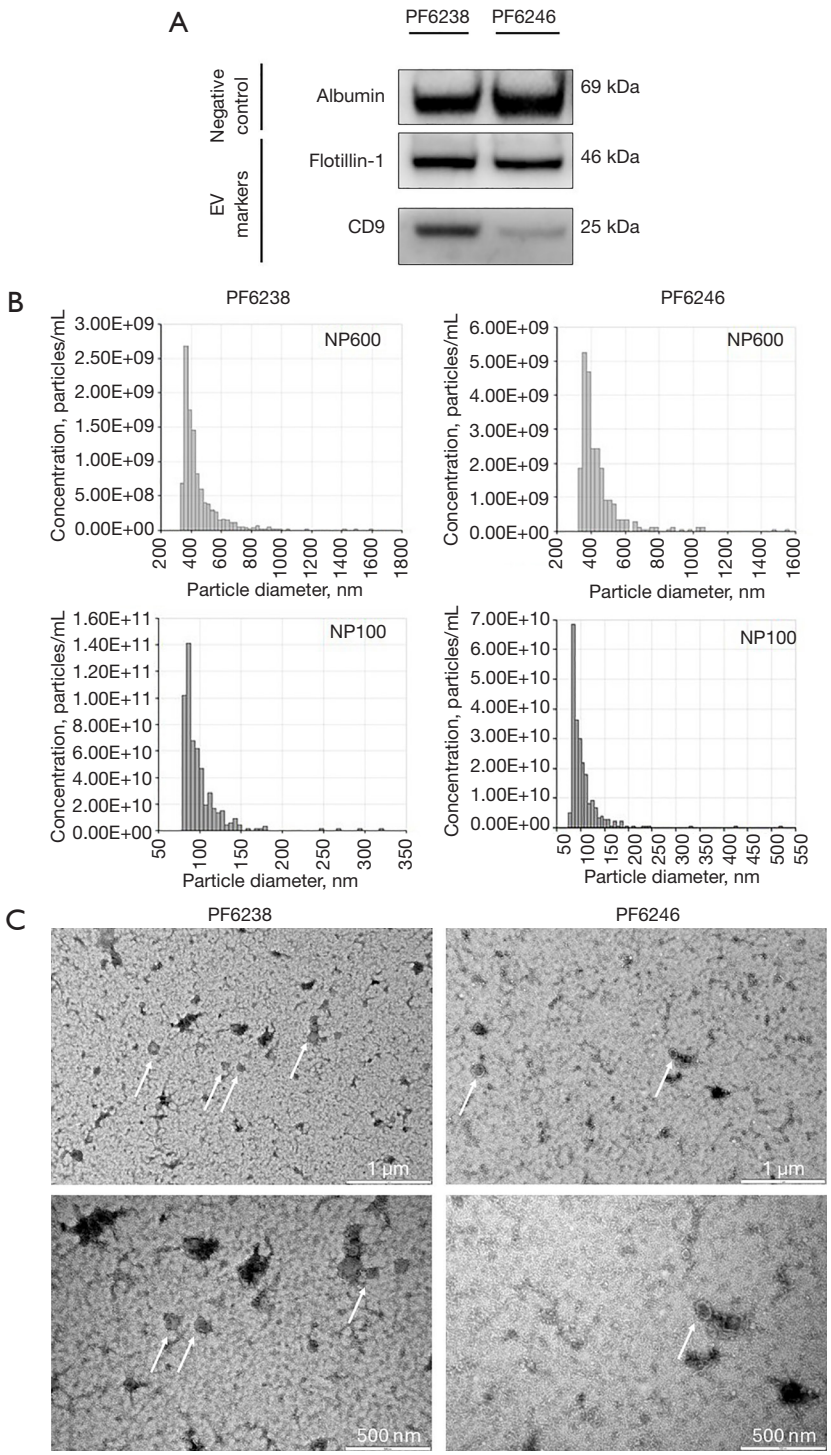

Figure 1 Characterisation of PFEV isolated from PF6238 and PF6246. (A) Western blotting analysis in PFEV of PF6238 and PF6246 showed positive staining of EV-associated protein markers—flotillin-1 and CD9 (positive markers) and albumin (negative marker) at varying intensities. (B) TRPS analysis showed an overall particle size distribution ranged at 80–520 nm for PFEV of PF6238 and PF6246, analysed with NP600 and NP100 using The Exoid analyser. (C) TEM images showed the presence of EV in PF6238 and PF6246 with cup-shaped morphology, as indicated by the white arrows, at image resolution of 1 µm and 500 nm, respectively. EVs, extracellular vesicles; PFEV, pleural fluid extracellular vesicle; TRPS, tunable resistive pulse sensing; TEM, transmission electron microscopy.

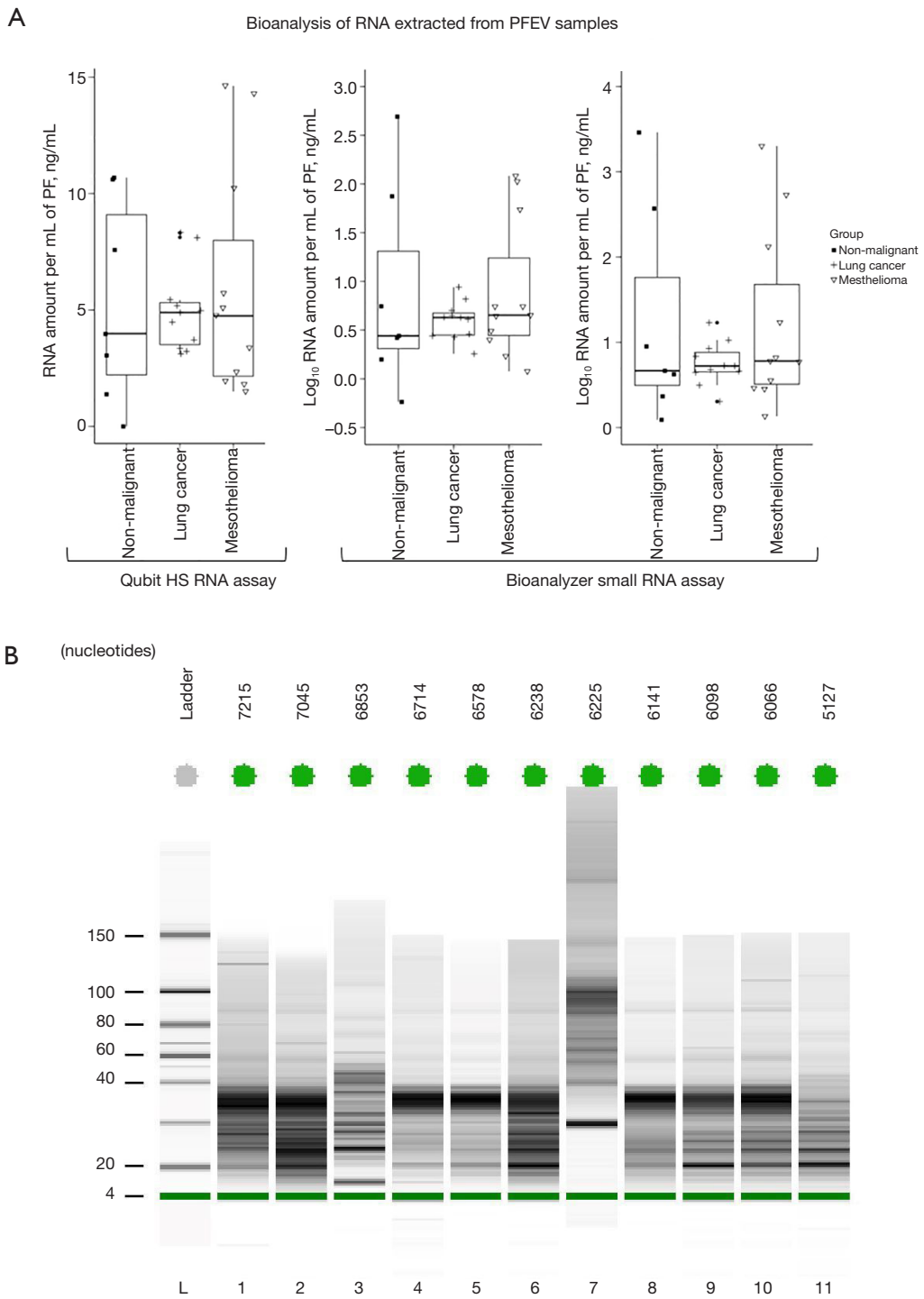

Figure 2 Bioanalysis of RNA extracted from PFEV. (A) Boxplots show the quantitation of RNA measured by Qubit HS RNA assay (left), and Bioanalyzer Small RNA assay (middle and right) expressed as $\log_{10}$ transformed values, extracted from 29 PFEV samples and stratified by diagnosis. (B) Bioanalyzer electrograms of ten randomly selected PFEV samples showed band sizes between 4 and 150 nucleotides at varying intensities. PF, pleural fluid; PFEV, pleural fluid extracellular vesicle; HS, high sensitivity; L, ladder.

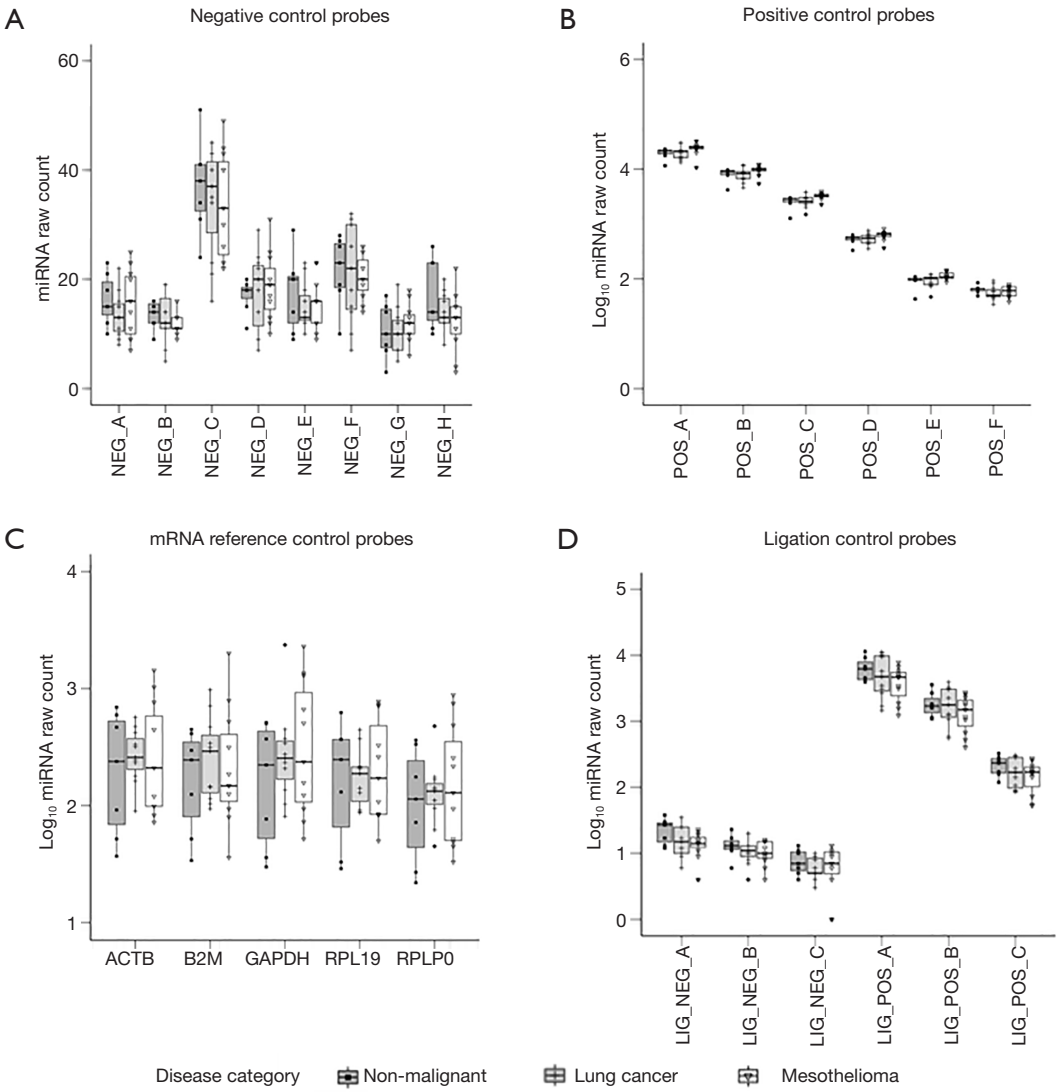

Figure 3 Overall performance of Nanostring nCounter® miRNA expression assay in PFEV (n=29). (A) Eight negative control probes (NEG_A to NEG_H) show relatively low level of expression. (B) Positive control probe A–F (POS_A to POS_F) showed consistent loading of input amount and minimal lane-to-lane variation. (C) mRNA reference control probes (ACTB, B2M, GAPDH, RPL19, RPLP0) showed varying expression levels amongst the 29 PFEV samples. (D) Ligation negative control probe A–C (LIG_NEG_A to LIG_NEG_C) show low expression levels, whereas linear expression levels were observed from ligation positive control probe A–C (LIG_POS_A to LIG_POS_C). miRNA, microRNA; PFEV, pleural fluid extracellular vesicle.

and RPLP0 (*Figure 3C*). Small RNA ligation controls supplied at concentrations of 128, 32, 8, 2, 0.5, and 0.125 fM were analysed to monitor ligation efficiency. Linear expression of ligation positive control probes A–C was observed in all samples, whereas ligation negative control probes A–C showed negligible expression, indicating minimal non-specific ligation (*Figure 3D*).

PFEV miRNA profiling

Nanostring miRNA raw counts were compared pairwise according to diagnosis in DESeq2, showing that a total of 32 PFEV-derived miRNAs were differentially expressed between NM and malignant effusions at unadjusted P<0.05 and $\log_2$fold change values ≥1.0. Based on Benjamini-Hochberg adjusted P, six of the 32 miRNAs were

Table 2 PFEV miRNAs differentially expressed in benign and MPE

miRNA	Malignant *vs.* NM†		metLUAD *vs.* NM†		MPM *vs.* NM†		MPM *vs.* metLUAD†	
	Log_2fold change	Adjusted P value	Log_2fold change	Adjusted P value	Log_2fold change	Adjusted P value	Log_2fold change	Adjusted P value
hsa-miR-145-5p	−1.53	0.003	−1.38	0.03	−1.71	0.004		
hsa-miR-1246			4.75	0.02			−7.85	<0.001
hsa-miR-141-3p			1.63	0.02			−1.54	0.005
hsa-miR-200c-3p			2.86	<0.001			−2.39	<0.001
hsa-miR-9-5p			1.78	0.02				
hsa-miR-136-5p							1.78	0.02

Four comparison analyses of PFEV samples were performed using DESeq2: malignant *vs.* NM; metLUAD *vs.* NM, MPM *vs.* NM, MPM *vs.* metLUAD. Six miRNAs (hsa-miR-145-5p, hsa-miR-1246, hsa-miR-141-3p, hsa-miR-200c-3p, hsa-miR-9-5p, and hsa-miR-136-5p) were found to be significantly different at adjusted P<0.05 and log_2fold change values ≥1.0, and the direction of difference relative to the reference group marked by a symbol "†" is shown as higher (positive number) or lower (negative number). hsa-miR-145-5p levels were higher in NM than in malignant (including metLUAD and MPM) PFEVs. hsa-miR-1246, hsa-miR-141-3p, hsa-miR-200c-3p, and hsa-miR-9-5p levels were higher in metLUAD than in NM PFEV. Also, hsa-miR-1246, hsa-miR-141-3p, hsa-miR-200c-3p levels were significantly higher in metLUAD than in MPM. hsa-miR-136-5p levels were higher in MPM than in NM or metLUAD PFEVs. PFEV, pleural fluid extracellular vesicle; miRNA, microRNA; MPE, malignant pleural effusion; NM, non-malignant; metLUAD, lung adenocarcinoma metastatic to pleura; MPM, malignant pleural mesothelioma.

significantly different between various causes of pleural effusions, at adjusted P<0.05 and log_2fold change values ≥1.0 (*Table 2*). *Figure 4* shows boxplots of normalised miRNA expression in PFEV for these six miRNAs: hsa-miR-145-5p, hsa-miR-1246, hsa-miR-141-3p, hsa-miR-200c-3p, hsa-miR-9-5p, and hsa-miR-136-5p.

Benign *vs.* malignant effusions

hsa-miR-145-5p was the most significantly different miRNA between NM and malignant PFEV (adjusted P=0.003 to 0.03). The level of hsa-miR-145-5p expression was consistently higher in PFEVs from NM effusions than from malignant effusions. Log_2fold change values for pairwise comparisons were −1.53 (NM *vs.* malignant), −1.38 (NM *vs.* metLUAD) and −1.71 (NM *vs.* MPM) (*Table 2*).

metLUAD *vs.* benign effusions

Five miRNAs (hsa-miR-145-5p, hsa-miR-1246, hsa-miR-141-3p, hsa-miR-200c-3p, and hsa-miR-9-5p) differed significantly between NM and metLUAD effusions. Except for hsa-miR-145-5p, each was expressed at a higher level in metLUAD than in NM PFEVs (adjusted P<0.001 to P=0.02; *Table 2*). hsa-miR-1246 and hsa-miR-200c-3p displayed the greatest magnitudinal differences (log_2fold change values 4.75 and 2.86, respectively).

MPM *vs.* benign effusions

One miRNA, has-miR-145-5p, was significantly different between these samples, its expression higher in benign than in MPM PFEVs, adjusted P=0.003 (*Table 2*).

Mesothelioma *vs.* metLUAD

In malignant effusions PFEV, levels of hsa-miR-1246, hsa-miR-141-3p, and hsa-miR-200c-3p were significantly higher in effusions due to metLUAD than in those due to MPM (adjusted P<0.001 to P=0.005; log_2fold change values of −7.85, −1.54, and −2.39, respectively), while level of hsa-miR-136-5p were greater in effusions due to MPM than metLUAD (adjusted P=0.02; log_2fold change 1.78; *Table 2*).

Discussion

Presentation with pleural effusion may occur in a diverse range of NM conditions such as pneumonia, congestive heart failure, pulmonary embolism, and infections, as well as malignant conditions, including those arising from pleura itself, lung, breast, or other primary sites. Initial assessment of pleural effusion includes clinical history and examination, imaging, and pleural fluid analyses consisting of biochemistry, microbiology, and cytology. Digital pathology incorporating artificial intelligence systems offers

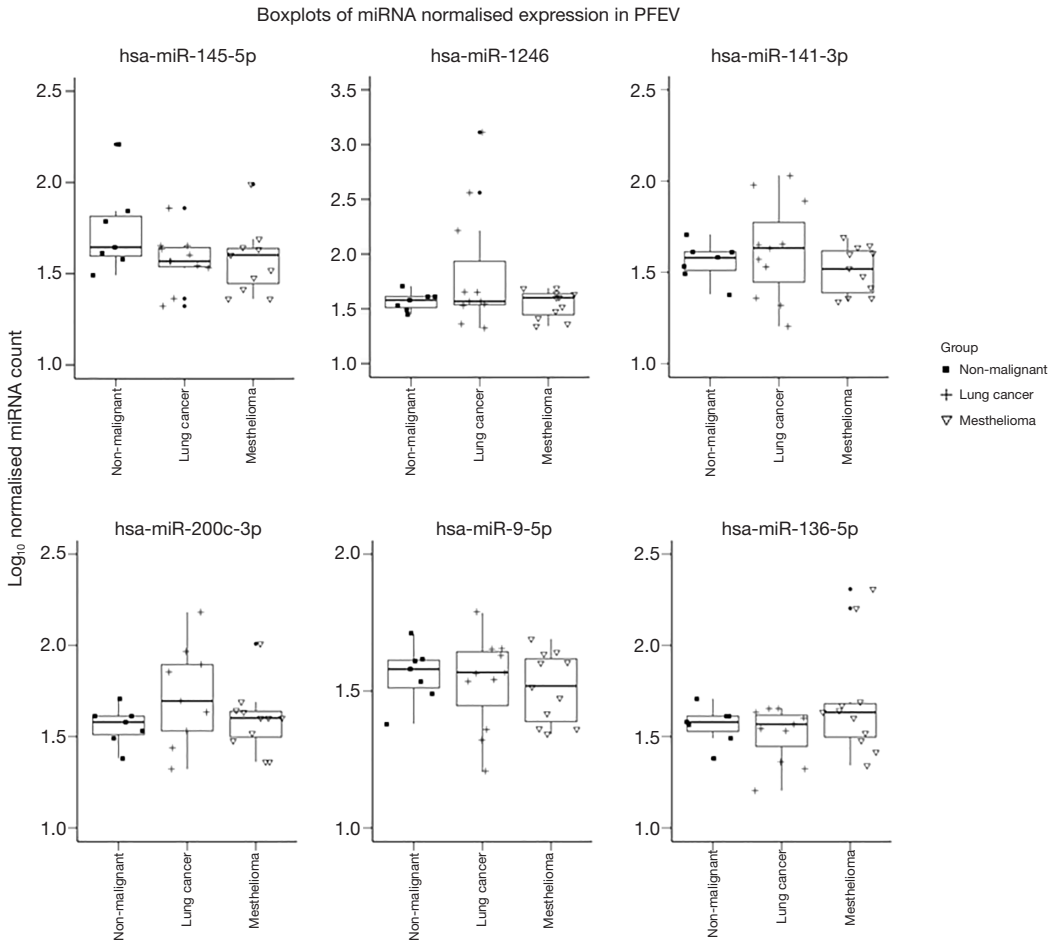

Figure 4 Boxplots showing normalised expression data of six PFEV miRNAs. Normalised expression counts of the six miRNAs that were significantly different between NM and malignant (metLUAD, MPM) effusions are shown. Note that Y-axis range and log base differ for each miRNA to simplify graphical presentation. miRNA, microRNA; PFEV, pleural fluid extracellular vesicle; NM, non-malignant; metLUAD, lung adenocarcinoma metastatic to pleura; MPM, malignant pleural mesothelioma.

advances to conventional light microscopy examination, with whole slide imaging allowing for simultaneous viewing of images at different locations and by multiple users, as well as unlimited annotations with specific tags on regions of interest (15). A recent meta-analysis evaluating the adoption of mobile devices into digital pathology in cytology demonstrated substantial concordance between conventional light microscopy and digital pathology with the use of mobile devices such as smartphones, tablets, and mobile apps (16). Nonetheless, further improvement in sample preparation, examination techniques, technology and validation are required before digital pathology can be widely accepted and adopted in clinical practice.

Malignancy is confirmed by the presence of malignant cells in pleural fluid, but it is not excluded if these are not present. Definitive diagnosis frequently requires repeated pleural fluid sampling, trans-thoracic needle biopsy, thoracoscopy, or other invasive measures. Tumour markers may aid differential diagnosis but lack consistency in distinguishing between NM and malignant etiology, as well as between primary pleural and metastatic causes of effusions. Carcinoembryonic antigen (CEA), carbohydrate antigen 15-3 or 19-9 (CA15-3/CA19-9), and a fragment of cytokeratin 19 (CYFRA 21-1) are some pleural fluid tumour markers that differentiate MPE, with high specificity (over 90%), but low sensitivity (~50%) (17). Immunocytochemistry testing of BAP1 and p16 deletion may support a diagnosis of MPM, yet MPM remains as

the most challenging effusion to diagnose by cytology, with overall test sensitivity at 0–46%, compared to higher sensitivity (up to 93%) for lung or breast cancer metastatic to pleura (18,19).

Pleural fluid miRNA profiles or specific miRNAs derived within the cellular or EV fractions have been previously reported to differentiate between malignant and benign pleural effusions (20). Differential expression analysis of miRNA in pleural fluids has been primarily studied for ability to differentiate between metastatic lung and non-MPE, identifying miRNAs such as miR-205-5p, miR-200b, miR-150-5p, and many others as potential biomarker candidates (11,20,21). Tumour-derived EVs facilitate tumorigenesis by interacting between tumour, normal and stromal cells (22), to exert both immunosuppressive (pro-tumoral) and anti-tumoral functions through mechanisms involving various types of immune cells and regulatory proteins (23). In malignant effusions, selectively packaged EV-components such as miRNAs both reflect and influence tumour growth, apoptosis, and cancer metastasis (24,25). Thus, miRNA derived from EV cargo of pleural fluid presents as a potential bioresource for novel biomarker discovery.

In this study, miRNA expression profiles in the EV fraction of pleural effusions were interrogated by Nanostring nCounter® miRNA expression assays. First, we verified the presence of EVs in extracts of pleural fluid obtained from two sequential high-speed ultracentrifugation steps following recommended techniques outlined in Minimal Information for Studies of Extracellular Vesicles 2018 (MISEV2018) (5). Then, as the internal controls embedded in the Nanostring assays fell within expected parameters, the feasibility of employing the highly sensitive Nanostring nCounter® miRNA expression assay to profile miRNAs derived from the PFEV fraction was demonstrated.

We identified potential positive miRNA biomarker candidates for benign pleural effusions (hsa-miR-145-5p), malignant effusions due to metLUAD (hsa-miR-1246, hsa-miR-141-3p, hsa-miR-200c-3p, and hsa-miR-9-5p), and malignant effusions due to mesothelioma (hsa-miR-136-5p). These miRNA candidates could be explored further as a single biomarker candidate to differentiate different pleural effusion diseases or to be tested simultaneously in a panel to complement current pleural effusion cytological testing. Suppression of hsa-miR-145-5p levels in the PFEV fraction of malignant effusions (MPM and metLUAD) compared with benign effusions is consistent with another report of lower levels of this miRNA in lung adenocarcinoma than in cancer-free lung tumour tissue (26).

The three PFEV miRNAs (hsa-miR-1246, hsa-miR-200c-3p, and hsa-miR-141-3p), whose expression levels were significantly elevated in metLUAD compared to NM and MPM PFEV are of interest for their potential as positive markers of pleural effusion due to metLUAD. It was previously reported that expression of hsa-miR-1246 in serum exosomes of non-small cell lung cancer (NSCLC) patients was higher than in healthy or NM respiratory disease controls (27). A microarray study of formalin-fixed, paraffin-embedded (FFPE) tumour demonstrated greater expression of hsa-miR-200c in adenocarcinomas (including the lung) than in MPM (28), and it was previously reported that levels of both miR-200c-3p and miR-141-3p in pleural effusion exosomes were higher in metLUAD than in effusions due to tuberculosis or other benign conditions (29,30). However, another study found that although levels of hsa-miR-141-3p in unfractionated serum were higher in early NSCLC than in controls, there was no significant difference in levels of hsa-miR-141-3p in the exosomal compartment (31).

In malignant effusions due to metLUAD, we found exosomal hsa-miR-9-5p levels to be higher than in NM effusions, raising the possibility that levels of exosomal hsa-miR-9-5p may be able to distinguish between malignant and benign effusions. This is supported by other studies showing higher expression of miR-9-5p in serum from patients with NSCLC compared to cancer-free controls (32), in cultured lung adenocarcinoma cells than in human bronchial epithelial cells (33,34), and in tumours themselves compared to corresponding normal tissue (35,36).

From our findings, hsa-miR-136-5p is of interest for its potential to distinguish effusions due to MPM from those due to metLUAD. Using a non-exposed human malignant mesothelioma cell line (JU77) as a comparator, Filetti *et al.* reported that expression of hsa-miR-136-5p was downregulated in JU77 cells exposed to 10 μg/mL fluoro-edenite fibres (37), suggesting a possible pathogenetic role of hsa-miR-136-5p in mesothelioma.

EV-derived miRNAs are known to play pivotal roles in cancer biology, acting as a tumour suppressor or oncogenes. In some instances, a single miRNA possesses dual roles depending on tumour stage, type of cancer, localisation within the cellular and extracellular environment, or other attributes such as smoking status, environmental exposure (38). The level of certain miRNAs in PFEV could reflect tumour stage, whereby late-stage cancers,

such as lung cancer metastatic to the pleura use EV export as a disposal mechanism to remove tumour-suppressive miRNAs, and thus promote local tumour progression and metastasis (39).

hsa-miR-145, hsa-miR-141-3p, and hsa-miR-200c have been reported as tumour suppressors for many cancers, including lung cancer and MPM. Intriguingly, their expression levels were vastly different between benign and malignant effusions, as observed in our study. hsa-miR-145 acts as a tumour suppressor in many cancers, with low expression often observed in cancer compared to NM control tissue (40-42). These studies point to a potential explanation for our observations of its low exosomal expression in malignant effusions. In contrast, despite the generally higher expression of hsa-miR-141-3p in liquid biopsies in cancer compared with NM states (29,31), there has been a report of lower expression in NSCLC tumour than in adjacent "non-tumour" tissue (43). Similarly, miR-141-3p was lower in MPM cells (NCI-H226, NCI-H2452, and MSTO-211H) than in NM mesothelial cells (Met-5A) (44). miR-141-3p belongs to the miR-200 family, and low expression of miRNAs in this family has been observed in cells undergoing epithelial-mesenchymal transition (29). However in some cancers, high levels of miRNAs in the miR-200 family were associated with advanced cancer stage (29). For example, high levels of miR-141 derived from plasma exosomes and serum were associated with more advanced cancer stage in small-cell lung cancer, and a potential mechanism by which exosomal miR-141 promotes tumour angiogenesis via EV cargo in establishing early metastatic niche was proposed (45). Another study found that high expression of miR-200c and miR-141 conferred shorter survival in NSCLC, also citing the angiogenic property of miR-141 in cancer biology (46). These previously reported findings are consistent with our observation of high hsa-miR-141-3p and hsa-miR-200c in PFEV due to metLUAD but not in benign effusions, and support the need for future studies to investigate how these miRNAs could potentially be involved in the metastatic process of lung cancer.

Several limitations to the study should be acknowledged. Firstly, this study was designed as an exploratory approach to evaluate the performance of the Nanostring nCounter® miRNA expression assay to profile miRNAs isolated from the hitherto less studied EV fraction of pleural fluid. It was not powered to determine whether any specific miRNA or miRNA profile was able to differentiate between diseases of the pleura, thus significantly limit the generalizability of the proposed PFEV miRNA candidates to differentiate between benign pleural effusion and MPE. Much larger purpose-designed studies would be needed for that aim. In this study, we show proof of principle that the composition of the EV compartment of pleural effusion fluid can be efficiently isolated and analysed for miRNA content, providing a methodologic pathway for these larger studies. Although the findings are suggestive of possible diagnostic utility for differentially expressed miRNAs, the small number of samples studied together with lack of representation of the whole spectrum of pleural diseases prohibit drawing definitive conclusions. MPE could also arise from cancer in breast, stomach, kidney, ovary, colon, lymphoma, and other lung cancer subtypes (squamous cell carcinoma, large cell carcinoma, etc.), of which had not been included in our study. We are aware of recent studies suggesting that differential miRNA expression can be attributed to differences in sex (male *vs.* female) (47) and age (young *vs.* older participants) (48), and acknowledge limited scope in our small study to properly account for these factors. Secondly, miRNA expression in PFEV could be altered by long–term sample storage and processing steps such as freeze-thaw cycles (49). A cohort of fresh pleural fluid samples analysed in real-time would ideally be used to determine diagnostic utility. Nevertheless, we have demonstrated that HS methods can detect EV miRNAs in stored samples. Finally, this initial study did not directly compare miRNA repertoires between PFEV and other bio-compartments such as pleural fluid supernatant, pleural fluid cellular compartment, or plasma. In future studies, this analysis would be important to ensure that the most accessible, least invasive, and most cost-effective method of detecting disease-related changes in EV miRNAs is used.

Conclusions

Standard diagnostic tests based on cellular and supernatant fractions of pleural effusion currently have suboptimal diagnostic test characteristics for the diagnosis of pleural disease, especially in differentiating MPM from other malignancies metastatic to the pleura such as lung and breast cancers. This can lead to delayed diagnosis and treatment, and often a need for multiple invasive procedures to obtain diagnostic tissue. Selective packaging of EV cargo suggests that this compartment may be enriched in tumour markers. Results from this study show that miRNAs within the EV compartment of pleural fluid could be useful for studying differential expression related to disease

processes, and that PFEV miRNAs could represent a novel bioresource for improving pleural effusion-based diagnostic accuracy in the future.

Acknowledgments

The authors express gratitude to patients of The Prince Charles Hospital who donated pleural fluid for this study, and thank co-workers who contributed to this project.

Footnote

Reporting Checklist: The authors have completed the MDAR reporting checklist. Available at https://tlcr.amegroups.com/article/view/10.21037/tlcr-24-945/rc

Data Sharing Statement: Available at https://tlcr.amegroups.com/article/view/10.21037/tlcr-24-945/dss

Peer Review File: Available at https://tlcr.amegroups.com/article/view/10.21037/tlcr-24-945/prf

Funding: This work was supported by the Common Good (The Prince Charles Hospital Foundation) under the Innovation Grant (No. INN2018-17), the Emerging Research Grant (No. EM2018-08), and the PhD Scholarship (No. PhD2014-01).

Conflicts of Interest: All authors have completed the ICMJE uniform disclosure form (available at https://tlcr.amegroups.com/article/view/10.21037/tlcr-24-945/coif). K.M.F. serves as an unpaid editorial board member from August 2023 to July 2025. The other authors have no conflicts of interest to declare.

Ethical Statement: The authors are accountable for all aspects of the work in ensuring that questions related to the accuracy or integrity of any part of the work are appropriately investigated and resolved. The present study was directed in accordance with the guidelines of the Declaration of Helsinki (as revised in 2013). All specimens were acquired through The Prince Charles Hospital Lung Bank (approval number: HREC/17/QPCH/54), approved by the Metro North Health Human Research Ethics Committee. This study, including approval to access the specimens collected through The Prince Charles Hospital Lung Bank, was approved by the Metro North Health Human Research Ethics Committee (approval number: LNR/2019/QPCH/52409) and The University of Queensland Human Research Ethics Committee (approval number: 2019001147/HREC/52409) and informed consent was taken from all the patients.

References

1. Miller LJ, Holmes IM, Lew M. An Updated Contextual Approach to Mesothelial Proliferations in Pleural Effusion Cytology Leveraging Morphology, Ancillary Studies, and Novel Biomarkers. Arch Pathol Lab Med 2024;148:409-18.
2. Orlandi R, Cara A, Cassina EM, et al. Malignant Pleural Effusion: Diagnosis and Treatment-Up-to-Date Perspective. Curr Oncol 2024;31:6867-78.
3. Lepus CM, Vivero M. Updates in Effusion Cytology. Surg Pathol Clin 2018;11:523-44.
4. Loveland P, Christie M, Hammerschlag G, et al. Diagnostic yield of pleural fluid cytology in malignant effusions: an Australian tertiary centre experience. Intern Med J 2018;48:1318-24.
5. Théry C, Witwer KW, Aikawa E, et al. Minimal information for studies of extracellular vesicles 2018 (MISEV2018): a position statement of the International Society for Extracellular Vesicles and update of the MISEV2014 guidelines. J Extracell Vesicles 2018;7:1535750.
6. Welsh JA, Goberdhan DCI, O'Driscoll L, et al. Minimal information for studies of extracellular vesicles (MISEV2023): From basic to advanced approaches. J Extracell Vesicles 2024;13:e12404.
7. Guo S, Wang X, Shan D, et al. The detection, biological function, and liquid biopsy application of extracellular vesicle-associated DNA. Biomark Res 2024;12:123.
8. Zhu M, Gao Y, Zhu K, et al. Exosomal miRNA as biomarker in cancer diagnosis and prognosis: A review. Medicine (Baltimore) 2024;103:e40082.
9. Zhao W, Cao XS, Han YL, et al. Diagnostic utility of pleural cell-free nucleic acids in undiagnosed pleural

effusions. Clin Chem Lab Med 2022;60:1518-24.
10. Mlika M, Zorgati MM, Abdennadher M, et al. The diagnostic performance of micro-RNA and metabolites in lung cancer: A meta-analysis. Asian Cardiovasc Thorac Ann 2024;32:45-65.
11. Lin J, Wang Y, Zou YQ, et al. Differential miRNA expression in pleural effusions derived from extracellular vesicles of patients with lung cancer, pulmonary tuberculosis, or pneumonia. Tumour Biol 2016. [Epub ahead of print]. doi: 10.1007/s13277-016-5410-6.
12. Cheerla N, Gevaert O. MicroRNA based Pan-Cancer Diagnosis and Treatment Recommendation. BMC Bioinformatics 2017;18:32.
13. Chee TM, O'Farrell HE, Lima LG, et al. Optimal isolation of extracellular vesicles from pleural fluid and profiling of their microRNA cargo. J Extracell Biol 2023;2:e119.
14. Love MI, Huber W, Anders S. Moderated estimation of fold change and dispersion for RNA-seq data with DESeq2. Genome Biol 2014;15:550.
15. Eccher A, Girolami I. Current state of whole slide imaging use in cytopathology: Pros and pitfalls. Cytopathology 2020;31:372-8.
16. Santonicco N, Marletta S, Pantanowitz L, et al. Impact of mobile devices on cancer diagnosis in cytology. Diagn Cytopathol 2022;50:34-45.
17. Zheng WQ, Hu ZD. Pleural fluid biochemical analysis: the past, present and future. Clin Chem Lab Med 2023;61:921-34.
18. Chang CH, Ost DE. Malignant pleural disease: a pragmatic guide to diagnosis. Curr Opin Pulm Med 2022;28:282-7.
19. Kaul V, McCracken DJ, Rahman NM, et al. Contemporary Approach to the Diagnosis of Malignant Pleural Effusion. Ann Am Thorac Soc 2019;16:1099-106.
20. Sorolla MA, Sorolla A, Parisi E, et al. Diving into the Pleural Fluid: Liquid Biopsy for Metastatic Malignant Pleural Effusions. Cancers (Basel) 2021;13:2798.
21. Roman-Canal B, Moiola CP, Gatius S, et al. EV-associated miRNAs from pleural lavage as potential diagnostic biomarkers in lung cancer. Sci Rep 2019;9:15057.
22. Tao SC, Guo SC. Role of extracellular vesicles in tumour microenvironment. Cell Commun Signal 2020;18:163.
23. Scholl JN, Dias CK, Muller L, et al. Extracellular vesicles in cancer progression: are they part of the problem or part of the solution? Nanomedicine (Lond) 2020;15:2625-41.
24. Mohammadi S, Yousefi F, Shabaninejad Z, et al. Exosomes and cancer: From oncogenic roles to therapeutic applications. IUBMB Life 2020;72:724-48.
25. Kalluri R, LeBleu VS. The biology, function, and biomedical applications of exosomes. Science 2020;367:eaau6977.
26. Jiang W, Zhang C, Kang Y, et al. The roles and mechanisms of the circular RNA circ_104640 in early-stage lung adenocarcinoma: a potential diagnostic and therapeutic target. Ann Transl Med 2021;9:138.
27. Huang D, Qu D. Early diagnostic and prognostic value of serum exosomal miR-1246 in non-small cell lung cancer. Int J Clin Exp Pathol 2020;13:1601-7.
28. Benjamin H, Lebanony D, Rosenwald S, et al. A diagnostic assay based on microRNA expression accurately identifies malignant pleural mesothelioma. J Mol Diagn 2010;12:771-9.
29. Wang Y, Xu YM, Zou YQ, et al. Identification of differential expressed PE exosomal miRNA in lung adenocarcinoma, tuberculosis, and other benign lesions. Medicine (Baltimore) 2017;96:e8361.
30. Hydbring P, De Petris L, Zhang Y, et al. Exosomal RNA-profiling of pleural effusions identifies adenocarcinoma patients through elevated miR-200 and LCN2 expression. Lung Cancer 2018;124:45-52.
31. Wu Q, Yu L, Lin X, et al. Combination of Serum miRNAs with Serum Exosomal miRNAs in Early Diagnosis for Non-Small-Cell Lung Cancer. Cancer Manag Res 2020;12:485-95.
32. Yang Y, Chen K, Zhou Y, et al. Application of serum microRNA-9-5p, 21-5p, and 223-3p combined with tumor markers in the diagnosis of non-small-cell lung cancer in Yunnan in southwestern China. Onco Targets Ther 2018;11:587-97.
33. Zhu K, Lin J, Chen S, et al. miR-9-5p Promotes Lung Adenocarcinoma Cell Proliferation, Migration and Invasion by Targeting ID4. Technol Cancer Res Treat 2021;20:15330338211048592.
34. Zhang TX, Duan XC, Cui Y, et al. Clinical significance of miR-9-5p in NSCLC and its relationship with smoking. Front Oncol 2024;14:1376502.
35. Mitra R, Edmonds MD, Sun J, et al. Reproducible combinatorial regulatory networks elucidate novel oncogenic microRNAs in non-small cell lung cancer. RNA 2014;20:1356-68.
36. Li G, Wu F, Yang H, et al. MiR-9-5p promotes cell growth and metastasis in non-small cell lung cancer through the repression of TGFBR2. Biomed Pharmacother 2017;96:1170-8.
37. Filetti V, Lombardo C, Loreto C, et al. Small RNA-Seq

Transcriptome Profiling of Mesothelial and Mesothelioma Cell Lines Revealed microRNA Dysregulation after Exposure to Asbestos-like Fibers. Biomedicines 2023;11:538.
38. Otmani K, Lewalle P. Tumor Suppressor miRNA in Cancer Cells and the Tumor Microenvironment: Mechanism of Deregulation and Clinical Implications. Front Oncol 2021;11:708765.
39. Mills J, Capece M, Cocucci E, et al. Cancer-Derived Extracellular Vesicle-Associated MicroRNAs in Intercellular Communication: One Cell's Trash Is Another Cell's Treasure. Int J Mol Sci 2019;20:6109.
40. Kadkhoda S, Ghafouri-Fard S. Function of miRNA-145-5p in the pathogenesis of human disorders. Pathol Res Pract 2022;231:153780.
41. Qiu ZK, Yang E, Yu NZ, et al. The biomarkers associated with epithelial-mesenchymal transition in human keloids. Burns 2024;50:474-87.
42. Tekin SS, Erdal ME, Asoğlu M, et al. Biomarker potential of hsa-miR-145-5p in peripheral whole blood of manic bipolar I patients. Braz J Psychiatry 2022;40:378-87.
43. Li W, Cui Y, Wang D, et al. MiR-141-3p functions as a tumor suppressor through directly targeting ZFR in non-small cell lung cancer. Biochem Biophys Res Commun 2019;509:647-56.
44. Wang P, Bai C, Shen S, et al. MALAT1 promotes malignant pleural mesothelioma by sponging miR-141-3p. Open Med (Wars) 2021;16:1653-67.
45. Mao S, Lu Z, Zheng S, et al. Exosomal miR-141 promotes tumor angiogenesis via KLF12 in small cell lung cancer. J Exp Clin Cancer Res 2020;39:193.
46. Tejero R, Navarro A, Campayo M, et al. miR-141 and miR-200c as markers of overall survival in early stage non-small cell lung cancer adenocarcinoma. PLoS One 2014;9:e101899.
47. Tomeva E, Krammer UDB, Switzeny OJ, et al. Sex-Specific miRNA Differences in Liquid Biopsies from Subjects with Solid Tumors and Healthy Controls. Epigenomes 2023;7:2.
48. Giordano M, Boldrini L, Servadio A, et al. Differential microRNA expression profiles between young and old lung adenocarcinoma patients. Am J Transl Res 2018;10:892-900.
49. Ahmadian S, Jafari N, Tamadon A, et al. Different storage and freezing protocols for extracellular vesicles: a systematic review. Stem Cell Res Ther 2024;15:453.

Cite this article as: Chee TM, Zahra CJ, Fong KM, Yang IA, Bowman RV. Potential utility of miRNAs derived from pleural fluid extracellular vesicles to differentiate between benign and malignant pleural effusions. Transl Lung Cancer Res 2025;14(1):124-138. doi: 10.21037/tlcr-24-945